ORIGINAL RESEARCH

Fast and Reliable Synthesis of Melanin Nanoparticles with Fine-Tuned Metal Adsorption Capacities for Studying Heavy Metal Ions Uptake

Eman R Darwish[1–4]
Haitham Kalil[1,2,5]
Wafa Alqahtani[1,2]
Sayed MN Moalla[4]
Nasser M Hosny[4]
Alaa S Amin[6]
Heidi B Martin[3]
Mekki Bayachou[1,2]

[1]Department of Chemistry, Cleveland State University, Cleveland, OH, USA; [2]Lerner Research Institute, Cleveland Clinic, Cleveland, OH, USA; [3]Department of Chemical & Biomolecular Engineering, Case Western Reserve University, Cleveland, OH, USA; [4]Chemistry Department, Faculty of Science, Port Said University, Port Said, Egypt; [5]Chemistry Department, Faculty of Science, Suez Canal University, Ismailia, Egypt; [6]Chemistry Department, Faculty of Science, Benha University, Benha, Egypt

Purpose: Adsorption and uptake of heavy metals by polymeric nanoparticles is driven by a variety of physicochemical processes. In this work, we examined heavy metal uptake by synthetic melanin nanoparticles and analyzed physicochemical properties that affect the extent of metal uptake by the nanoparticles.

Methods: Eumelanin nanoparticles were synthesized in a one-pot fast process from a 5,6-diacetoxy indole precursor that is hydrolyzed in situ into dihydroxy indole (DHI). The method allows the possibility of changing the level of sodium ions that ends up in the nanoparticles. Two variants of synthetic DHI–melanin (low-sodium and high sodium variants) were evaluated and demonstrated different relative adsorption efficiencies for heavy metal cations.

Results and Discussion: For the low-sodium DHI–melanin and in terms of percentages of metal ion removal, the relative order of extraction from 50 ppm solutions was $Zn^{2+} > Cd^{2+} > Ni^{2+} > Co^{2+} > Cu^{2+} > Pb^{2+}$, with the extraction percentages ranging from 90% down to 76%, for a 30-minute adsorption time before equilibrium. The lower-sodium DHI–melanin consistently removed more Zn^{2+} than the higher-sodium variant. Electron microscopy (SEM) showed an increase in melanin particle size after metal ions uptake. In addition, X-ray photoelectron spectroscopy (XPS) of DHI–melanin particles with depth profiling after Zn ions uptake supported particle swelling and ion transport within the particles.

Conclusion: These initial studies showed the potential of this straightforward synthesis to obtain synthetic DHI–melanin nanoparticles similar to those from biological sources with the possibility to fine-tune their metal adsorption capacity. These synthetic nanoparticles can be used either for the removal of a variety of metal ions or to mimic and study mechanisms of metal uptake by melanin deriving from biological sources, with the potential to understand, for instance, differential heavy metal uptake by various melanic pigments.

Keywords: one-pot synthesis, melanin nanoparticles, differential sodium content, heavy metals, adsorption, metal extraction

Introduction

In their 2019 report on drinking water, sanitation, and hygiene, the World Health Organization and the United Nations reported that globally, over 2 billion people still rely on unsafe water.[1] Also, over 85% of countries reported that they do not have sufficient financial resources to implement adequate sanitation plans for drinking water. The situation is expected to deteriorate by 2025 since half of the world's population is expected to be living in water-stressed areas.[1] Adequate

Correspondence: Mekki Bayachou
Department of Chemistry, Cleveland State University, 2399 Euclid Ave, Cleveland, OH, 44115, USA
Email m.bayachou@csuohio.edu

101

supply of safe drinking water is essential for all people regardless of their social or economic conditions. An important environmental factor that compromises the safety of water is the presence of heavy metals.[2] Globally, it is estimated that 24% of all disease burden and an estimated 23% of all deaths are attributable to environmental factors including exposure to heavy metals.[3] Estimated 4.9 million deaths worldwide (8.3% of total mortality) were linked to environmental exposure from chemical mismanagement.[4,5] Many developing countries are facing a growing crisis of heavy metal contamination in waterways exceeding limits permitted by the World Health Organization (WHO), due to increased discharges of heavily polluted industrial and domestic wastewater.[6,7] For instance, the industrial sector in the Greater Cairo area in Egypt is adding more pesticides, nutrients, and heavy metals into the Nile River, which is the main water source to this densely populated area.[8]

Heavy metals can contaminate the water either as dissolved ions or suspended particles, thus requiring multiple strategies for their removal. Four general classifications of remediation techniques have been reported: (a) chemical precipitation, (b) coagulation with flocculation, (c) membrane filtration, and (d) adsorption.[7] Chemical precipitation removes dissolved ions by chemical reactions that convert them into insoluble hydroxides, sulfides or carbonates, for subsequent filtration; hydroxide precipitation at high pHs is the most widely used due to lower cost and simplicity.[9] Although this method is the most effective at higher metal concentrations, it is generally not sufficient to achieve the required water quality standards for safe reuse.[10,11] In addition, since raising the pH is the primary way of inducing precipitation for this method, the number of affordable reagents may limit the scope of the method.

The coupled coagulation-flocculation process is another large-scale purification method used to precipitate suspended colloids. It often uses metal compounds (eg alum, aluminum chloride, iron chloride and iron sulfate) as inorganic coagulants along with various high molecular weight polymeric coagulation aids.[12–15] As in chemical precipitation, some metal ions can interfere with the aggregation of others in coagulation methods applied to mixtures of ions. However, these two methods remain affordable and more scalable than other methods, such as membrane filtration technologies.[16,17] Membrane filtration technologies use passive exclusion methods or active electrodialysis to selectively remove ions from mixtures.[18] In addition to cost, membrane methods must also overcome other operational hurdles, such as pressure drop and fouling.

Adsorption is an efficient and low-cost method for removal of metal ions or particles. This approach is versatile and uses a variety of interfaces taking advantage of both physical and chemical interactions.[19] The most common adsorption methods are adsorption on activated carbon,[20–22] as well as on natural or synthetic polymers.[23–27] Inexpensive powders and natural feedstocks and waste products have also been used in adsorption methods either as such or after conversion to activated carbons.[25]

Melanins are a family of polymeric bio-pigments found in many parts of the human body including the hair, skin, and eyes,[28–30] and are known to bind a variety of inorganic and organic species.[31–35] Two broad melanin classes or moieties with structural heterogeneity, the brown-black eumelanin and the reddish-yellow pheomelanin, are found naturally or can be synthesized.[36–39] These polymeric scaffolds have important chelating interactions with metal ions both in vivo and in vitro.[40–43] Some early work on both natural and synthetic melanin explored the nature of metal-ion binding sites over a range of pH.[44,45] For the case of synthetic melanin in particular, this work identified the number and nature of chelating sites as a function of pH and the melanin precursor.[45]

Metals play an integral role in the formation of melanin supramolecular structures, and these structures are capable of binding or trapping metal ions. These natural scaffolds were therefore explored for metal and/or bacteria removal from water.[46] Natural melanin from squid ink displayed higher adsorption capacity than other materials for lead removal.[40] Eumelanin synthesized by polymerization of L-DOPA was shown to remove >95% of Pb^{2+} and was better than the natural melanin extracted from human hair;[34] more modest adsorption rates (50 to 90%) were observed for Cu^{2+}, Zn^{2+}, and Cd^{2+}. Removal rates of Cr (VI) varied with the natural melanin source.[47] The collective work on melanin-like scaffolds indicates that these materials provide important substrates that can be chemically fine-tuned to optimize adsorption of heavy metals from aqueous solutions. In this paper, we use a new synthetic eumelanin from polymerized dihydroxy indole to explore the affinity of a series of heavy metals to this nanoscale synthetic network. We also shed light on how a subtle change in the chemical makeup of this synthetic

polymer affects the affinity and selective removal of metal ions.

Results and Discussion
Synthetic DHI–Melanin Characterization

Two categories of melanin nanoparticles were synthesized as described in the experimental section (see Supporting Information): low sodium melanin (referred to as LSM) and high sodium melanin (referred to as HSM). In keeping with the general definitions and practical classification of various kinds of melanin,[39] we will use the term "DHI-melanin" for the synthetic melanin used in this work. For convenience, the terms "LSM melanin" and "HSM melanin" throughout this work also mean the synthetic "DHI-melanin" material. The synthesis procedure is adapted from a previous work in our lab involving a DAI precursor in an organic-water co-solvent mixture, but not using electro-polymerization.[48] Other procedures in the literature[33] reported the synthesis of melanin-like polymers in 6 hours using a DL-dopa precursor. A similar procedure using DAI was reported in the literature,[37] but also reported the same 6-hour time span of the reaction in strictly aqueous solution. Extraction of natural melanin (eg from *Marine Pseudomonas sp.*) requires even longer times in excess of 72 hours.[38] Our method, taking less than 30 minutes to complete, is faster and yields samples with reproducible quality.

The scanning electron microscopy images of our LSM melanin as synthesized here showed nanoparticle-like features with an estimated particle size of about 190 nm, Figure 1A.

The nanoparticle-like features of our synthetic melanin are distinctly different from synthetic samples reported by Costa et al for amorphous solids.[37] Likewise, Simon et al reported earlier synthetic samples prepared from L-dopa characterized by SEM as essentially amorphous solids with no discernable microstructures.[49] The amorphous synthetic melanin reported by others is likely the result of the strict aqueous medium in which these syntheses were conducted. Both L-dopa- and 5,6-diacetoxyindole-derived syntheses were conducted in water with no organic co-solvent.[37,49] As described in the experimental section, our synthesis was conducted in a mixture of water-ethanol. This is a critical difference from previous syntheses carried out in water-only solutions. In fact, it is well established that the mole fraction of ethanol in water-ethanol mixtures affects the partial molal volume of water.[50] In particular, in the mole fraction range between 0.08 and 0.1 of ethanol, it was shown that the structuredness of the

water-ethanol mixture reaches its maximum as a result of the optimal hydrogen bonding network of water molecules at this composition. Interestingly, our synthesis was carried out in a water-ethanol mixture in which ethanol's mole fraction ($\chi_{ethanol}$ =0.093) is within this optimal window. The nanoparticle aspect of the synthetic melanin that we report here is likely the result of the specific physico-chemical behavior of the solvent mixture which, in this case, not only helps the oxidative polymerization of melanin but also shapes the growth of resulting nanoparticles. Another property that may be critical to our synthesis is the reducing power of alcohol. Primary and secondary alcohols by themselves are known to behave as reducing agents.[51,52] In our case, the interplay between the oxidative growth of the synthetic melanin polymer and the reducing power of the ethanol results in the growth of the observed nanospheres rather than the amorphous solid observed under strictly aqueous solutions. The effect of the water-ethanol as co-solvents that we observe here has precedent. Previous literature reports show that the unique feature of water-ethanol mixtures at the optimal partial molal volume of water and optimal hydrogen bonding also proved to be very useful in accelerating the synthesis of other kinds of nanoparticles.[53] Although not related to this paper, it is important to mention that the electrochemical polymerization of DHI on electrodes under similar water-ethanol conditions also results in melanin films with similar nanoparticle features (see Supporting Information Figure S1). Interestingly, the nanosphere particles observed in our synthetic samples following our co-solvent protocol are similar to those reported for samples of natural eumelanin from *S. Officinalis*.[49] Recent atomic force microscopy characterization of morphologies of natural eumelanin from various cephalopods also reported similar features of spherical nanoparticles with size distribution in the 20–250 nm range.

EDS analysis confirmed the presence of carbon, nitrogen, oxygen consistent with the elemental composition of melanin. It also showed the presence of sodium, which is expected since our synthetic procedure uses NaOH in the hydrolysis of DAI, Figure 1B.

FTIR spectroscopy analysis of melanin particles is consistent with previous reports.[37] Our samples of synthetic melanin show three characteristic features (see Supporting Information Figure S2). The first feature at ~1581 cm^{-1}, is associated with carboxylate groups and nitrogen-containing heterocycles, as well as aromatic
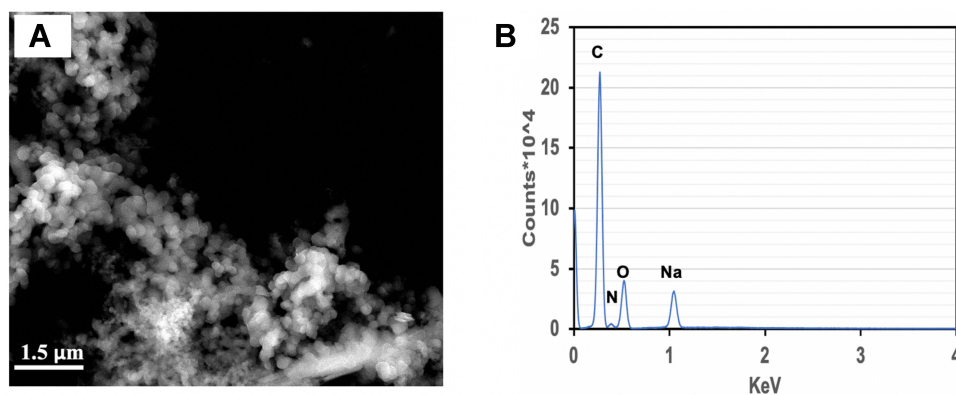
Figure 1 Characterization of synthetic melanin nanoparticles by SEM and elemental analysis. (**A**) The micrograph shows melanin nanoparticles with an average particle size of 190 nm for LSM sample; SEM of HSM (not shown) exhibited similar characteristics. (**B**) Energy dispersive X-ray spectroscopy confirmed the expected atomic composition of carbon, nitrogen, oxygen and sodium.

C=C bond in the polymeric framework. The second band at ~1354 cm^{-1} is representative of o-hydroxy quinone groups. Finally, a third peak at ~3333 cm^{-1} is associated with catechol groups.

Characterization of Metal Cations Within the Melanin Nanoparticles

We also characterized the melanin particles after exposure and adsorption of various metal cations. We found that in general the melanin particle size, as estimated from SEM, increases with nominal diameter after adsorption of metal ions, Figure 2. This is true for all metals used (Zn^{2+}, Cd^{2+}, Ni^{2+}, Co^{2+}, Cu^{2+} or Pb^{2+}). It is important to note that the reported diameter sizes for the melanin nanoparticles with adsorbed metals are not absolute-per-particle sizes, but rather relative nominal sizes determined from the SEM analysis of nanoparticle aggregates shown in the micrographs. Metal ion extraction from polymeric adsorbents, such as melanin, is mediated mainly through the interaction of metal ions with functional groups in the network.[54] In this case, catechol and quinone-imine groups, and the indole's π cloud, all are potential interaction sites for the metal ion. The complexation of metallic ions at the surface and the potential exchange with inner sites within the polymeric network of the nanoparticles are expected to affect the estimated average size of the particles after metal extraction.

Fourier Transform IR analysis of the synthetic melanin samples after interaction with metal ions gives evidence of the uptake of ions by the nanoparticles (see Supporting Information Figure S3 and Table S1 for measured wavenumbers before and after metal adsorption). In this regard, the peaks characteristic of carboxylate and quinone-imine groups

in melanin exhibit shifts to lower wavenumbers as a result of metal ion complexations, consistent with previous literature reports.[37] The notable increase in intensity of vibrations of CC and CO featured in peak A as well as those of catechol groups is indicative of metal complexations.[55] The splitting of peak B in the presence of Co^{2+} ions into a double band is likely an indication of two distinct binding modes of cobalt ions which would generate two distinct stretching modes of C-O in the catechol groups. Metal incorporation into the melanin nanoparticle network was also confirmed using EDS (Supporting Information, Figure S3).

We also used X-ray photoelectron spectroscopy (XPS) with depth profiling to measure differences in the elemental composition of the melanin nanoparticles, particularly in terms of metal ion content at different depths. Figure 3 shows representative survey scans at two nominal depths from the surface of synthesized LSM melanin nanoparticles after exposure and uptake of Zn^{2+} ions from the solution.

The survey scans show the presence of Zn^{2+} ions both at the surface and within the synthetic melanin nanoparticles (eg the 2p^3 peak, 1022 keV binding energy). The XPS analysis also shows that standardized integral areas of zinc peaks increase from the surface of the nanoparticles to a nominal depth of 10 nm, indicating a relative enrichment of melanin particles with the metal ion. This is consistent with SEM analysis (see Figure 2), which showed a clear increase in the size of melanin nanoparticles after uptake of each divalent metal ion. This XPS finding supports a mechanism of metal uptake at the surface (through, for instance, ion exchange) and through diffusion within pores and interaction with binding sites using stepwise chelation/decomplexation within the catechol polymeric network of melanin. Catecholate complexes with divalent metal ions (eg
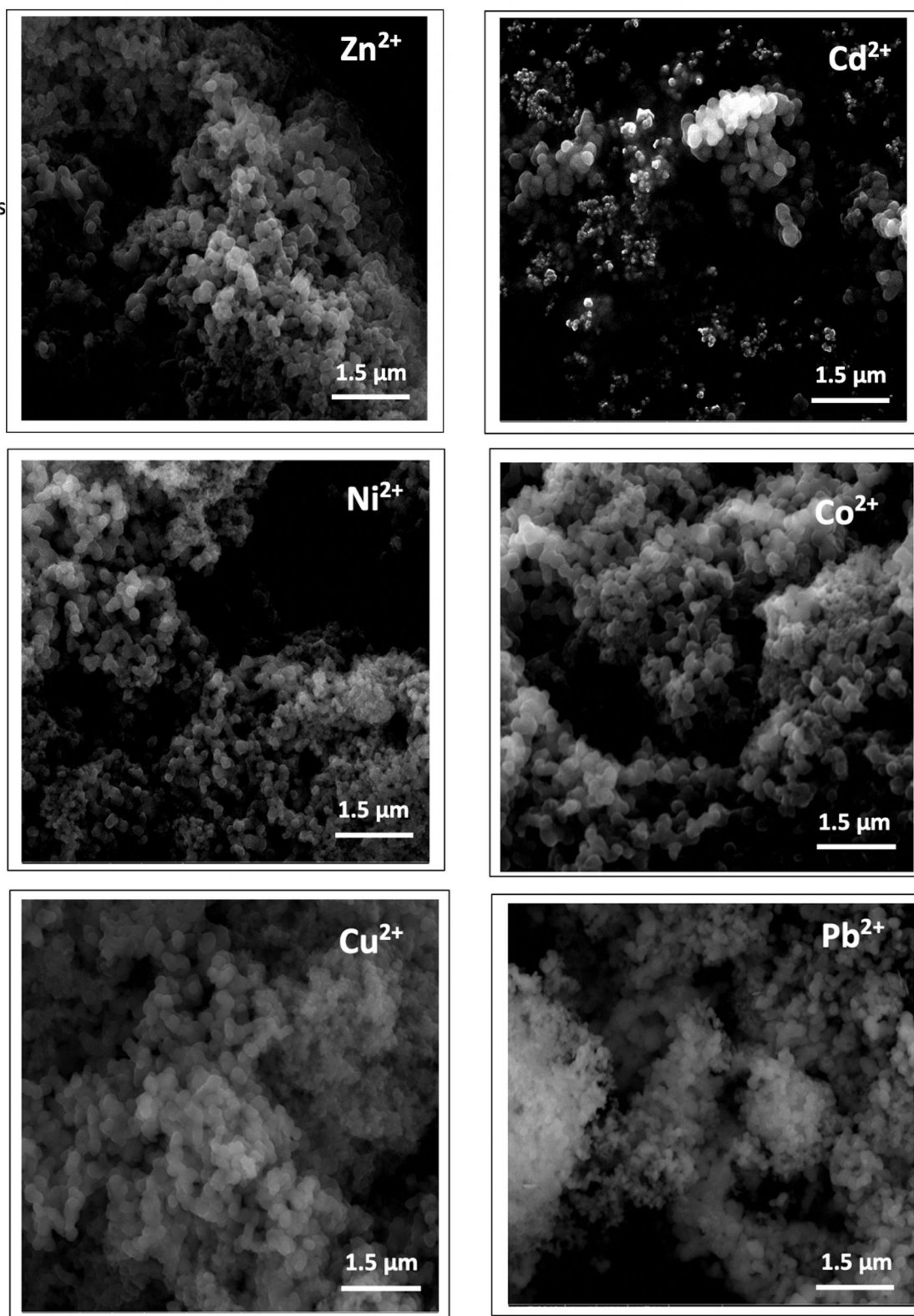
Figure 2 SEM micrographs of melanin nanoparticles showed a general increase in particle size after extraction of metal divalent cations from aqueous solutions. The metal ion symbol on each micrograph indicates the metal ion adsorbed. The estimated particle size after adsorption of the metal ions are as follows: Zn^{2+} 200 nm, Cd^{2+} 300 nm, Ni^{2+} 220 nm, Co^{2+} 225 nm, Cu^{2+} 230 nm, and Pb^{2+} 240 nm.
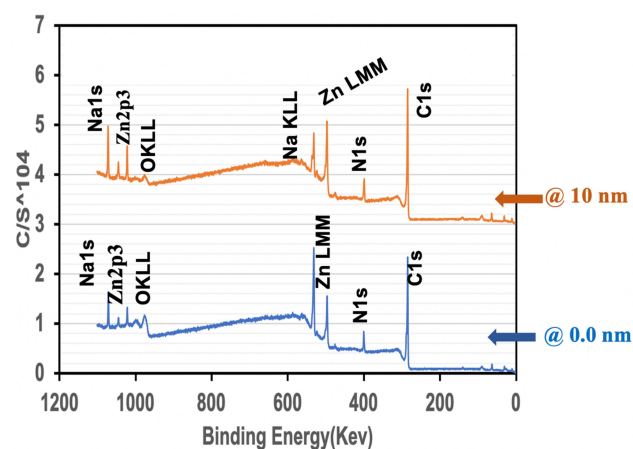
Figure 3 XPS survey spectrum of synthetic melanin nanoparticles after uptake of Zn^{2+} ions (exposure to 50 ppm starting concentration). Survey spectra taken with sputtering at nominal depths of 0 and 10 nm to monitor zinc ions.

Zn^{2+}, Ni^{2+}, Co^{2+}, Cu^{2+}) are known to form both mono- and bis-metal–ligand species.[56] The dynamic interconversion of mono- and bis-catecholates (possibly mixed with the involvement of quinone-imine groups) is expected to facilitate the metal uptake and transport process in the polymeric network within the melanin nanoparticles.

Metal Ion Extractions from Aqueous Solutions

We used ICP to monitor and quantify the uptake of metal ions by our synthetic melanin nanoparticles from aqueous solutions. In this regard, we constructed calibration curves for the six divalent metal ions (Zn^{2+}, Cd^{2+}, Ni^{2+}, Co^{2+}, Cu^{2+} and Pb^{2+}) in aqueous solutions.

The calibration curves used in this work are reported in supporting information (see Figure S4). We first used LSM melanin for metal ion extraction using 50 ppm starting metal ion concentrations over a 30-min extraction time. Figure 4 shows the extent of extraction of the various metal ions in aqueous solutions by LSM melanin nanoparticles. We measured both the amount of metal adsorbed on the nanoparticles and the amount of metal ions left in the solution using the methods described in the experimental section.

A general observation from Figure 4 is that uptake of zinc ions by the synthetic melanin nanoparticles is the highest (in terms of percent concentration uptake) among all divalent metal ions studied. The actual percentages of uptake for all metal ions based on ICP determinations are listed in Table 1.

We observe an almost 90% removal of Zn^{2+} ions from aqueous solutions, followed by Cd^{2+} ions (85.8%), Ni^{2+} (83.1%), Co^{2+} (82.0%), Cu^{2+} (80.2%), and finally Pb^{2+} ions
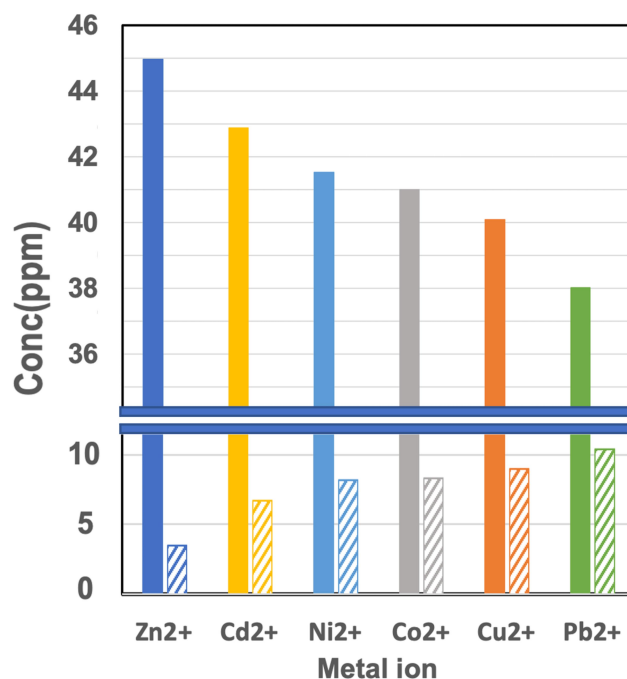

Figure 4 Concentration of metal ions after extraction from aqueous solution using LSM melanin (7 mg melanin, 50 ppm starting concentration). Concentrations were determined using ICP. Solid bars show the concentration of metal ions retrieved from the melanin nanoparticles after adsorption (uptake). Striped bars show the concentrations left in the supernatant after metal adsorption. A break in y-axis is introduced because of the difference in magnitudes between concentrations of uptake versus the concentrations left in the supernatant. The scale before and after the y-axis break is adjusted to reflect concentration differences.

exhibiting the lowest percentage of uptake, but still at a reasonable level of 76%. It is important to note that ICP measurements account for almost 100% of the starting ion concentration, since the % amount of metal left in the supernatant solution is complementary to the % amount adsorbed on the melanin nanoparticles for all metal ions used in this work, Table 1.

The percentages of metal uptake under our conditions can be converted to standardized adsorption capacities in

Table 1 Metal Ion Percentages of the Overall Uptake by Synthetic Melanin Using ICP Measurements

Metal Ion	% Metal Amount Uptake in Melanin Nanoparticles	% Metal Amount Left in Solution
Zn^{2+}	89.9	7.07
Cd^{2+}	85.8	13.3
Ni^{2+}	83.1	16.4
Co^{2+}	82.0	16.6
Cu^{2+}	80.2	16.6
Pb^{2+}	76.0	20.7

Notes: Percentages are based on a 30-minute ion capture from 50 ppm starting concentrations using 7 mg synthetic melanin.

mmol/g in order to compare and contrast the performance of synthetic melanin in this work with other adsorbents.

Table 2 lists adsorption capacities of melanin for the various metal ions along with values reported for other adsorbents. While the values we report here were not necessarily optimized and are not equilibrium data, the performance of melanin nanoparticles as prepared in this work is very promising for heavy metal removal and outperforms traditional adsorbents, such as some forms of activated carbon as well as some commercial resins and zeolite. We note the promising performance of melanin nanoparticles not only in terms of adsorption capacity but also in terms of speed of uptake.

In addition to the sorbent cases mentioned in Table 2, our preliminary findings with the new melanin nanoparticles show better removal rates for Cu^{2+}, Ni^{2+} and Zn^{2+} compared to other sorbents, such as polymer-grafted silica systems.[27] In all literature cases examined, we observed that melanin nanoparticles exhibit significantly higher removal capacity of Zn^{2+} ions.

A number of physicochemical mechanisms can be at play in determining the extent and the order of adsorption of heavy metals on a given adsorbent. These may include ion-exchange, chelation and coordination, complex formation, surface electrostatic interaction, or a combination of some or all these mechanisms.[60]

In our case, and in terms of adsorption capacities, the uptake performance of melanin nanoparticles is highest for Zn^{2+}, Ni^{2+} and Co^{2+} metallic ions. The adsorption capacity is relatively low for Cu^{2+} and drops significantly for Cd^{2+} and Pb^{2+} ions.

Electronegativity, hydration radius, and effective ionic radius of metal ions have been used to rationalize trends in adsorption capacities. It is tempting to use the relatively large effective radii of Cd^{2+} and Pb^{2+} ions (95 pm and 119 pm, respectively) as a justification for the observed low adsorption capacities for these two metal ions on the melanin nanoparticles. While the size of the ion may play a role, electronegativity of the metal ions in solution may provide a better rationale (the solution-phase electronegativity scale[61] for metal ions in solution is very different from the classic Pauling electronegativity scale for elements). The electronegativity of metal ions in solution is likely an important driver of the interaction of the metal ions with the electron-donating chelation sites (catechol and quinone-imine groups) within the synthetic melanin nanoparticles. Figure 5 shows a plot of the measured adsorption capacities as a function of the solution-phase electronegativities of the metal ions taken from Reference.[61] The solution-phase electronegativities of the various metal ions seem to explain relatively well the ascent of the first part of the curve showing an increase in adsorption capacities as the electronegativity of the metal ion increases. Since the solution electronegativity of metal ions is key in their speciation and interaction with functional groups at the surface of nanoparticles and within the particles, it is not surprising that Pb^{2+} and Cd^{2+} ions with the lowest electronegativities in the group exhibit the lowest adsorption capacities. At the opposite end, Ni^{2+}, Co^{2+}, Zn^{2+}, and Cu^{2+} show higher adsorption capacities. However, it is clear that solution-phase electronegativity of metal ions alone does not explain the overall behavior since the ascending trend ceases after Ni^{2+} and a downturn is noticed.

Formation constants of catecholate complexes on the nanoparticles and the resulting metal-site strength are also at play. Knowing that the uptake of the metallic cations is ultimately driven by the interaction of binding sites on the

Table 2 Adsorption Capacities of Metal Ions in Millimole Ion per Gram of Adsorbent for Synthetic Melanin in This Work and for Other Adsorbents from Literature

Adsorbent	Adsorption Capacities (mmol/g)						Extraction/Contact Time	References
	Zn^{2+}	Cd^{2+}	Ni^{2+}	Co^{2+}	Cu^{2+}	Pb^{2+}		
Granular Activated Carbon[a]	–	0.01	–	–	0.04	0.03	24 hours	[57]
Powdered Activated Carbon[a]	–	0.01	–	–	0.05	0.12	24 hours	[57]
Zeolite	–	0.20	–	–	0.20	0.48	24 hours	[57]
Activated Carbon Fibers	–	–	0.152		0.174	0.147	24 hours	[58]
Duolite GT-73 Resin[a]	0.85	0.94	0.97	–	0.97	0.59	24 hours	[59]
Amberlite 200	1.3	2.0	1.5	–	1.4	1.7	24 hours	[59]
Melanin nanoparticles[b]	1.47	0.82	1.56	1.49	1.35	0.40[b]	30 minutes[b]	This work

Notes: [a]Initial concentrations in these reports were in the millimolar range and thus are higher than concentrations used in this work. Our numbers would be higher for similar concentrations; [b]Extraction/contact time in this work is not equilibrium time and the capacities reported are lower limit capacities in this case.
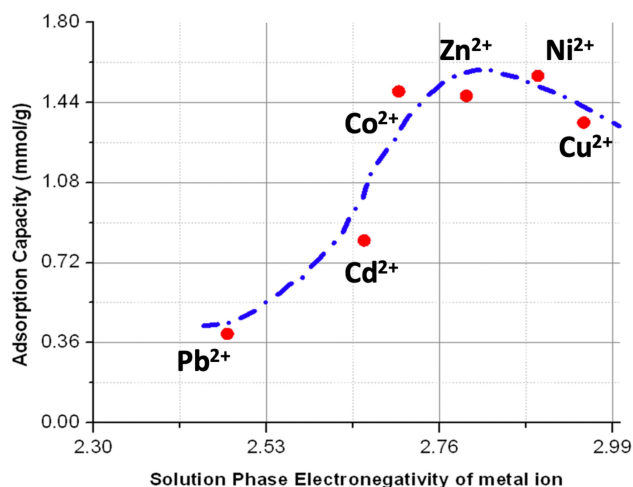
Figure 5 Plot of adsorption capacity as a function of solution-phase electronegativity of the various divalent metal ions. Adsorption capacity data is calculated from ICP measurements. Electronegativities that reflect metal ions in solution are different from the Pauling electronegativities data from Li et al.[61] Dashed blue curve is not from a model and is added to show the general trend only.

nanoparticles, a comparison of formation constants K_f for the complexation ($M^{2+} + L^{2-} \rightarrow$ M-L, where M^{2+} is the metal ion and L^{2-} is the chelating ligand at any site in the nanoparticle) can provide a rationale for the behavior observed. Given the structure and ligand content of melanin, ligand sites are mostly catechol groups. We therefore looked into the thermodynamic properties of divalent metal-catecholate complexes. Formation constants (ie a stability measure with respect to the free metal ions) of bivalent transition metal series with model catechol ligands have been determined.[62] Thermodynamic data on Pb-catechol complexes are not available but the formation constant of this complex is expected to be small based on a study that established a monodentate form of the complex.[63] Together, the following order in terms of increasing K_f can be used: Pb << Cd < Ni^{2+} ~ Co^{2+} < Zn^{2+}<< Cu^{2+}. Again, the overall order seems to correlate with the trend of adsorption capacities for these ions, but the rate of increase in adsorption capacity as a function of catechol complex formation is not maintained and the trend breaks down after Ni^{2+} (see Figure S5, Supporting Information). While a higher formation constant is needed for efficient binding of the metal ions and their uptake by the melanin nanoparticles, an extremely large constant is expected to be counterproductive. This would negatively affect the active transport of metal ions between binding sites within the adsorbing nanoparticles. For Cu^{2+} ions, the formation constant of the putative catechol complex is reported to be $K_f > 10^{12}$ for a model catechol

compound.[62] This may be the reason why the adsorbing capacity for copper ions is lower and the trend starts to decline after the maximum values observed for cobalt, zinc, and nickel ions. Again, while some level of thermodynamic stability of the complex is needed for increased adsorption, large formation constants can limit transport between sites within the particles, and thus can lower the overall capacity. Solution electronegativity of metal ions and catechol complex formation constants are expected to be synergistic and complementary for lower values; however, extremely large thermodynamic stabilities of the catechol-metal complex may be limiting in terms of adsorption capacity within melanin particles.

Sodium Content and Adsorption Capacity

Since the interaction with catecholate and other binding sites in melanin particles is the driving force for metal removal from solution, we examined whether the sodium ion content of the synthetic melanin nanoparticles affects the adsorption capacity. Our one-pot synthetic procedure uses NaOH during the hydrolysis step of DAI, which is a precursor of DHI that ultimately oxidizes into the polymeric melanin particles. Sodium ions are expected to be part of the deprotonated binding sites of the synthesized melanin prepared under essentially basic conditions. EDS characterization in Figure 1B indeed shows the presence of sodium ions in the melanin particles. We slightly modified the synthesis process of the melanin particles by increasing the mole equivalent of sodium hydroxide used in the hydrolysis of DAI by 20%, as described in the experimental section (See Supporting Information). This modified process resulted in a variant of melanin nanoparticles with a relatively higher sodium content (labeled HSM for High Sodium Melanin as opposed to LSM for the low sodium variant). We compared and contrasted the behavior of the two variants (LSM and HSM melanin particles) in terms of adsorption levels for Zn^{2+} ions over a 30-min time span. As in the first part of this work, we used the same amount of melanin particles and the same initial concentration of Zn^{2+} ions of 50 ppm. We measured the amount of Zn ions adsorbed using ICP. Figure 6 shows the Zn^{2+} adsorption levels for both low and high sodium melanin variants in mg of Zn per gram of melanin.

The LSM variant clearly shows a higher level of Zn^{2+} ions adsorption compared to HSM over the 30-min extraction time. We also performed XPS analysis with depth
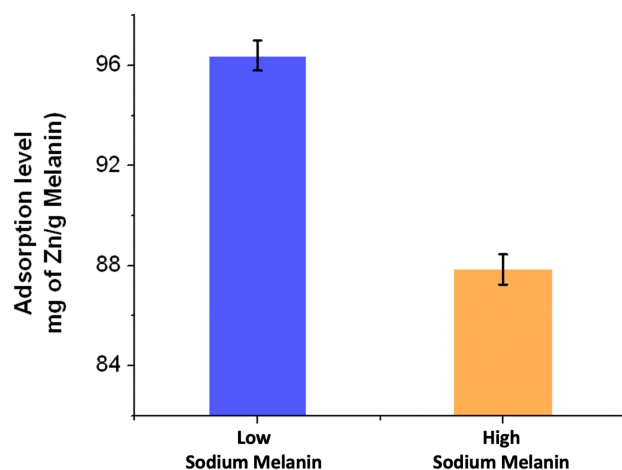
Figure 6 Adsorption capacities over a 30-min extraction time in milligrams of Zn adsorbed per gram of melanin adsorbent for LSM (blue bar) and HSM (orange bar) melanin variants. Error bars on the graph represent the 95% confidence interval based on 3 replicates and a standard deviation of 0.2 mg/g derived from ICP measurements.

profiling of the two melanin variants after adsorption of Zn ions in order to compare their profiles. We report in Table 3 the atomic composition ratios (Zn/C, Na/C, O/C and N/C) from XPS for both LSM and HSM adsorbents.

An overall observation of XPS atomic ratios data in Table 3 shows that the High Sodium Melanin (HSM) variant contains a higher level of sodium ions compared to the Low Sodium Melanin (LSM). The relatively higher sodium levels in HSM hold true both at the surface of the nanoparticles and at a 10-nm depth. Comparison of the Zn/C ratios in Table 3 indicates that LSM nanoparticles adsorb higher zinc content compared to HSM particles. The relatively higher content of Zn ions in LSM particles is observed both at the surface and deep within these particles at comparable levels. This finding is not surprising since it is consistent with the observed higher adsorption levels of zinc ions on the LSM adsorbent compared to the HSM variant under similar conditions as reported in Figure 6.

Table 3 Atomic Ratios from XPS with Depth Profiling at 0 and 10 nm from the Surface of the Melanin Nanoparticles

		O/C	N/C	Na/C	Zn/C
LSM melanin nanoparticles	@ 0.0 nm	0.303	0.061	0.041	0.012
	@ 10.0 nm	0.130	0.066	0.065	0.018
HSM melanin nanoparticles	@ 0.0 nm	0.364	0.086	0.055	0.003
	@ 10.0 nm	0.190	0.099	0.082	0.004

Notes: All ratios mentioned are for melanin samples after Zn adsorption.

The exact reason why the HSM variant adsorbs lower amounts of metal ions with respect to LSM is not exactly clear at this point, but it can be simply due to the fact that the excess sodium ions compete for and occupy the same binding sites as Zn^{2+} ions in this case, within the melanin particles. However, control experiments with preformed LSM particles suggest that exogenous sodium ions (ie preformed LSM melanin particles immersed in a solution of sodium ions) do not affect the heavy metal adsorption capacity of the melanin particles. Another potential reason may have to do with the nature of HSM particles: the relatively more basic conditions (20% mole equivalent to more of NaOH) under which the HSM particles are prepared likely result in a different organization of the heterogenous oligomers that aggregate to form the melanin nanoparticles during the synthesis. Sodium and other ions are known to provide bridging interactions in the melanin-like network (for instance, in our case, at the indole's nitrogen and catechol groups of the DHI units in the polymer). A higher sodium content will therefore result in a relatively rigid polymer network. On the other hand, it is established that melanin particles undergo reorganization to accommodate various metal ions.[37,64] Together, this may explain why the high sodium melanin particles show lower adsorption levels of metal ions compared to the low sodium melanin nanoparticles.

The one-pot melanin synthesis method in water-ethanol as co-solvents allowed us to prepare and characterize low-sodium and high-sodium melanin adsorbents that exhibit distinct profiles in terms of metal uptake. This preliminary study shows the versatility of the synthetic method in potentially preparing other variants and study how slight changes in structure or salt content can affect their metal uptake. Understanding how slight changes in melanin-like structures affect their uptake and accumulation of heavy metals may have implications for problems of biological importance, such as differential metal accumulation in melanic pigments in the brain.

Acknowledgments

Ibrahim and Shaimaa Maher for help with some control experiments. The funding support of the Egyptian Cultural Bureau is gratefully acknowledged. MB acknowledges partial funding from NIH grant EB019739 as well as FRD and USRA grants by CSU.

Disclosure

The authors declare that they have no conflicts of interest for this work and no known competing financial interests or personal relationships that could have appeared to influence the work reported in this paper.

References

1. UN-Water World Health Organization. National systems to support drinking-water, sanitation and hygiene: global status report 2019. UN-Water global analysis and assessment of sanitation and drinking-water (GLAAS) 2019 report. Geneva, Switzerland: World Health Organization; 2019.

2. World Health Organization. Cadmium in drinking-water: background document for development of WHO guidelines for drinking-water quality. Geneva: World Health Organization; 2004.

3. Prüss-üstün A, Corvalán C. Preventing disease through healthy environments. World Health Organization; 2006.

4. Mamtani R, Stern P, Dawood I, Cheema S. Metals and disease: a global primary health care perspective. *J Toxicol*. 2011;2011:319136. doi:10.1155/2011/319136

5. Prüss-üstün A, Vickers C, Haefliger P, Bertollini R. Knowns and unknowns on burden of disease due to chem- icals: a systematic review. *Environ Health*. 2010;10(1):1–15.

6. Youssef M, Morsy EM, Soliman SM, Abdel-Latief AR. Heavy metal pollutants in fresh water. *J Biomater*. 2018;2(2):46–50.

7. Goher ME, Ali MH, El-Sayed SM. Heavy metals contents in Nasser Lake and the Nile River, Egypt: an overview. *Egypt J Aquat Res*. 2019;49:301–312. doi:10.1016/j.ejar.2019.12.002

8. Lasheen M, El-Kholy G, Sharaby C, Elsherif I, El-Wakeel S. Assessment of selected heavy metals in some water treatment plants and household tap water in Greater Cairo, Egypt. *Manag Environ Qual Int J*. 2008;19(3):367–376. doi:10.1108/14777830810866473

9. AbiD BA, BrbootI MM, Al-ShuwaikI NM. Removal of heavy metals using chemicals precipitation. *J Eng Technol*. 2011;29(3):595–612.

10. Altaher H, Alghamdi A, Omar W. Innovative biosorbent for the removal of cadmium ions from wastwater. *Environ Eng Manag J*. 2015;14(4):793–800. doi:10.30638/eemj.2015.088

11. Abdel-Shafy HI. Chemical treatment for removal of heavy metals from industrial wastewater. *Egypt J Chem*. 2015;58(1):1–12.

12. Amuda O, Amoo I, Ipinmoroti K, Ajayi O. Coagulation/flocculation process in the removal of trace metals present in industrial wastewater. *JASEM*. 2006;10(3):159–162. doi:10.4314/jasem.v10i3.17339

13. Hargreaves AJ, Vale P, Whelan J, et al. Coagulation–flocculation process with metal salts, synthetic polymers and biopolymers for the removal of trace metals (Cu, Pb, Ni, Zn) from municipal wastewater. *Clean Technol Envir*. 2018;20(2):393–402. doi:10.1007/s10098-017-1481-3

14. Pang FM, Kumar P, Teng TT, Omar AM, Wasewar KL. Removal of lead, zinc and iron by coagulation–flocculation. *J Taiwan Inst Chem Eng*. 2011;42(5):809–815. doi:10.1016/j.jtice.2011.01.009

15. Johnson PD, Girinathannair P, Ohlinger KN, Ritchie S, Teuber L, Kirby J. Enhanced removal of heavy metals in primary treatment using coagulation and flocculation. *Water Environ Res*. 2008;80 (5):472–479. doi:10.2175/106143007X221490

16. Khulbe K, Matsuura T. Removal of heavy metals and pollutants by membrane adsorption techniques. *Appl Water Sci*. 2018;8(1):19. doi:10.1007/s13201-018-0661-6

17. El-Gendi A, Ali S, Abdalla H, Saied M. Microfiltration/ultrafiltration polyamide-6 membranes for copper removal from aqueous solutions. *Membr Water Treat*. 2016;7(1):55–70. doi:10.12989/mwt.2016.7.1.055

18. Lakherwal D. Adsorption of heavy metals: a review. *Int J Environ Res*. 2014;4(1):41–48.

19. Bobade V, Eshtiagi N. Heavy metals removal from wastewater by adsorption process: a review. Asia Pacific Confederation of Chemical Engineering Congress 2015: APCChE 2015, incorporating CHEMECA 2015. Engineers Australia; 2015.

20. Esmael AI, Matta ME, Halim HA, Azziz FMA. Adsorption of heavy metals from industrial wastewater using palm date pits as low cost adsorbent. *Int J Eng Adv Technol*. 2014;3:71–76.

21. Gupta VK, Ganjali M, Nayak A, Bhushan B, Agarwal S. Enhanced heavy metals removal and recovery by mesoporous adsorbent prepared from waste rubber tire. *Chem Eng J*. 2012;197:330–342. doi:10.1016/j.cej.2012.04.104

22. Zheng X, Yu N, Wang X, et al. Adsorption properties of granular activated carbon-supported titanium dioxide particles for dyes and copper ions. *Sci Rep*. 2018;8(1):6463. doi:10.1038/s41598-018-24891-1

23. Da Sacco L, Masotti A. Chitin and chitosan as multipurpose natural polymers for groundwater arsenic removal and As2O3 delivery in tumor therapy. *Mar Drugs*. 2010;8(5):1518–1525. doi:10.3390/md8051518

24. El-Kafrawy AF, El-Saeed SM, Farag RK, El-Saied HA, Abdel-Raouf ME. Adsorbents based on natural polymers for removal of some heavy metals from aqueous solution. *Egypt J Pet*. 2017;26 (1):23–32. doi:10.1016/j.ejpe.2016.02.007

25. Zhang Y, Xue Q, Li F, Dai J. Removal of heavy metal ions from wastewater by capacitive deionization using polypyrrole/chitosan composite electrode. *Adsorp Sci Technol*. 2019;37(3–4):205–216. doi:10.1177/0263617418822225

26. Sun DT, Peng L, Reeder WS, et al. Rapid, selective heavy metal removal from water by a metal–organic framework/polydopamine composite. *ACS Cent Sci*. 2018;4(3):349–356. doi:10.1021/acscentsci.7b00605

27. Sartore L, Dey K. Preparation and heavy metal ions chelating properties of multifunctional polymer-grafted silica hybrid materials. *Adv Mater Sci Eng*. 2019;2019:1–11. doi:10.1155/2019/7260851

28. Hong L, Simon JD. Physical and chemical characterization of iris and choroid melanosomes isolated from newborn and mature cows. *Photochem Photobiol*. 2005;81(3):517–523. doi:10.1562/2005-03-02-RA-453

29. Kollias N, Sayre RM, Zeise L, Chedekel MR. New trends in photobiology: photoprotection by melanin. *J Photochem Photobiol B*. 1991;9(2):135–160. doi:10.1016/1011-1344(91)80147-a

30. Slominski RM, Zmijewski MA, Slominski AT. The role of melanin pigment in melanoma. *Exp Dermatol*. 2015;24(4):258–259. doi:10.1111/exd.12618

31. Enochs WS, Petherick P, Bogdanova A, Mohr U, Weissleder R. Paramagnetic metal scavenging by melanin: MR imaging. *Radiology*. 1997;204(2):417–423. doi:10.1148/radiology.204.2.9240529

32. Hong L, Liu Y, Simon JD. Binding of metal ions to melanin and their effects on the aerobic reactivity. *Photochem Photobiol*. 2004;80 (3):477–481. doi:10.1562/0031-8655(2004)080<0477:BOMITM>2.0. CO;2

33. Kim DJ, Ju K-Y, Lee J-K. The synthetic melanin nanoparticles having an excellent binding capacity of heavy metal ions. *B Korean Chem Soc*. 2012;33(11):3788–3792. doi:10.5012/bkcs.2012.33.11.3788

34. Sono K, Lye D, Moore CA, Boyd WC, Gorlin TA, Belitsky JM. Melanin-based coatings as lead-binding agents. *Bioinorg Chem Appl*. 2012;2012:1–10. doi:10.1155/2012/361803

35. Szpoganicz B, Gidanian S, Kong P, Farmer P. Metal binding by melanins: studies of colloidal dihydroxyindole-melanin, and its complexation by Cu(II) and Zn(II) ions. *J Inorg Biochem*. 2002;89(1–2):45–53. doi:10.1016/s0162-0134(01)00406-8

36. Meng S, Kaxiras E. Theoretical models of eumelanin protomolecules and their optical properties. *Biophys J*. 2008;94(6):2095–2105. doi:10.1529/biophysj.107.121087

37. Costa TG, Younger R, Poe C, Farmer PJ, Szpoganicz B. Studies on synthetic and natural melanin and its affinity for Fe(III) ion. *Bioinorg Chem Appl*. 2012;2012:712840. doi:10.1155/2012/712840

38. Tarangini K, Mishra S. Production, characterization and analysis of melanin from isolated marine Pseudomonas sp. using vegetable waste. *Res J Eng Sci*. 2013;2278:9472.

39. d'Ischia M, Wakamatsu K, Napolitano A, et al. Melanins and melanogenesis: methods, standards, protocols. *Pigment Cell Melanoma Res*. 2013;26(5):616–633. doi:10.1111/pcmr.12121

40. Chen S, Xue C, Wang J, et al. Adsorption of Pb(II) and Cd(II) by squid ommastrephes bartrami melanin. *Bioinorg Chem Appl*. 2009;2009:901563. doi:10.1155/2009/901563

41. Zhang R, Fan Q, Yang M, et al. Engineering melanin nanoparticles as an efficient drug-delivery system for imaging-guided chemotherapy. *Adv Mater*. 2015;27(34):5063–5069. doi:10.1002/adma.201502201

42. Chen W, Hashimoto K, Omata Y, et al. Adsorption of molybdenum by melanin. *Environ Health Prev Med*. 2019;24(1):36. doi:10.1186/s12199-019-0791-y

43. Wang Z, Zou Y, Li Y, Cheng Y. Metal-containing polydopamine nanomaterials: catalysis, energy, and theranostics. *Small*. 2020;16(18):e1907042. doi:10.1002/smll.201907042

44. Sarna T, Froncisz W, Hyde JS. Cu2+ probe of metal-ion binding sites in melanin using electron paramagnetic resonance spectroscopy. II. Natural melanin. *Arch Biochem Biophys*. 1980;202(1):304–313. doi:10.1016/0003-9861(80)90431-2

45. Froncisz W, Sarna T, Hyde JS. Cu2+ probe of metal-ion binding sites in melanin using electron paramagnetic resonance spectroscopy. I. Synthetic melanins. *Arch Biochem Biophys*. 1980;202(1):289–303. doi:10.1016/0003-9861(80)90430-0

46. Le Na NT, Hoa PT, Thang ND. Natural melanin as a potential biomaterial for elimination of heavy metals and bacteria from aqueous solution. *VNU J Sci*. 2016;32(1S).

47. Cuong AM, Le Na NT, Thang PN, et al. Melanin-embedded materials effectively remove hexavalent chromium (Cr VI) from aqueous solution. *Environ Health Prev Med*. 2018;23(1):9. doi:10.1186/s12199-018-0699-y

48. Kalil H, Maher S, Bose T, Al-Mahmoud O, Kay C, Bayachou M. Synthetic melanin films as potential interfaces for peroxynitrite detection and quantification. *ECS Trans*. 2017;80(10):1447–1458. doi:10.1149/08010.1447ecst

49. Nofsinger JB, Forest SE, Eibest LM, Gold KA, Simon JD. Probing the building blocks of eumelanins using scanning electron microscopy. *Pigment Cell Res*. 2000;13(3):179–184. doi:10.1034/j.1600-0749.2000.130310.x

50. Manabe M, Koda M. The partial molal volumes of normal chain alcohols in water-ethanol mixtures at 25oC. *Bull Chem Soc Jpn*. 1975;48(8):2367–2371. doi:10.1246/bcsj.48.2367

51. Teranishi T, Hosoe M, Tanaka T, Miyake M. Size control of monodispersed Pt nanoparticles and their 2D organization by electrophoretic deposition. *J Phys Chem B*. 1999;103(19):3818–3827. doi:10.1021/jp983478m

52. Wang Y, Li X, Du F, Yu H, Jin B, Bai R. Use of alcohols as reducing agents for synthesis of well-defined polymers by AGET-ATRP. *Chem Commun*. 2012;48:2800–2802. doi:10.1039/c2cc17525h

53. Sudare T, Ueno T, Watthanaphanit A, Saito N. Accelerated nanoparticles synthesis in alcohol-water-mixture-based solution plasma. *Phys Chem Chem Phys*. 2015;17(45):30255–30259. doi:10.1039/c5cp05168a

54. Liu P, Borrell PF, Bozic M, Kokol V, Oksman K, Mathew AP. Nanocelluloses and their phosphorylated derivatives for selective adsorption of Ag(+), Cu(2+) and Fe(3+) from industrial effluents. *J Hazard Mater*. 2015;294:177–185. doi:10.1016/j.jhazmat.2015.04.001

55. Gulley-Stahl H, Hogan PA, Schmidt WL, Wall SJ, Buhrlage A, Bullen HA. Surface complexation of catechol to metal oxides: an ATR-FTIR, adsorption, and dissolution study. *Environ Sci Technol*. 2010;44(11):4116–4121. doi:10.1021/es902040u

56. Sever MJ, Wilker JJ. Visible absorption spectra of metal-catecholate and metal-tironate complexes. *Dalton Trans*. 2004;7:1061–1072. doi:10.1039/b315811j

57. An HK, Park BY, Kim DS. Crab shell for the removal of heavy metals from aqueous solution. *Water Res*. 2001;35(15):3551–3556. doi:10.1016/s0043-1354(01)00099-9

58. Kadirvelu K, Faur-Brasquet C, Cloirec PL. Removal of Cu(II), Pb(II), and Ni(II) by adsorption onto activated carbon cloths. *Langmuir*. 2000;16(22):8404–8409. doi:10.1021/la0004810

59. Vaughan T, Seo CW, Marshall WE. Removal of selected metal ions from aqueous solution using modified corncobs. *Bioresour Technol*. 2001;78(2):133–139. doi:10.1016/s0960-8524(01)00007-4

60. Virgen MD, Vázquez OF, Montoya VH, Gómez RT. Removal of heavy metals using adsorption processes subject to an external magnetic field. *Heavy Metals*. 2018;253.

61. Li K, Li M, Xue D. Solution-phase electronegativity scale: insight into the chemical behaviors of metal ions in solution. *J Phys Chem A*. 2012;116(16):4192–4198. doi:10.1021/jp300603f

62. Murakami Y, Nakamura K, Tokunaga M. Stability order in metal chelate compounds. I. 4-carboxy -and 4-sulfocatechol complexes. *Bull Chem Soc Jpn*. 1963;36(6):669–675. doi:10.1246/bcsj.36.669

63. Lapouge C, Cornard JP. Theoretical study of the Pb(II)–catechol system in dilute aqueous solution: complex structure and metal coordination sphere determination. *J Mol Struct*. 2010;969(1):88–96. doi:10.1016/j.molstruc.2010.01.047

64. Borghetti P, Goldoni A, Castellarin-Cudia C, et al. Effects of potassium on the supramolecular structure and electronic properties of eumelanin thin films. *Langmuir*. 2010;26(24):19007–19013. doi:10.1021/la102973u